First Takeoff of a Flying Microrobot With No Moving Parts

Daniel S. Drew
and Kristofer S. J. Pister
Berkeley Sensor and Actuator Center
University of California, Berkeley
Berkeley, California 94720
Email: ddrew73@berkeley.edu

***Abstract*—The preponderance of research into flying microrobots has focused on biomimetic flight mechanisms. In this work, we demonstrate an insect-scale robot capable of vertical takeoff using electrohydrodynamic thrust, a mechanism with no natural analogue. The 10mg, 1.8cm by 1.8cm "ionocraft" operates at about 2400 volts and has a thrust to weight ratio of approximately 10. Feasibility of using individually addressable thrusters in a quadcoptor-esque manner for attitude control is demonstrated qualitatively. A combination of design choices in the microfabricated silicon electrodes and a machine-fabricated external fixture allow for reproducible hand-assembly of the microrobot.**

I. Introduction

While autonomous or semi-autonomous flying robots (drones) are already poised to disrupt a multitude of industries including logistics and photography, we have only just begun to explore the possible uses for this technology. Flying microrobots open up a new application space where unobtrusiveness and fine data granularity are keys to success. It is possible to imagine a future where microrobots serve as the spiritual successor to the wireless sensor, acting as self-installing networks or self-directed diagnostic tools. The ability to batch fabricate microrobots at a low unit cost will enable us to use them as disposable, versatile swarms [1]. Current work toward this end largely involves pico air vehicles, defined as having a maximum takeoff mass of 500 mg or less and maximum dimensions of 5 cm or less, which have a unique set of scale-dependent challenges [2]. To date, research has largely focused on biologically inspired mechanisms, specifically flying insects like the bee, for inspiration [3] [4].

Biomimetic designs may succeed in replicating the agility of a flying insect, but the evolution of the flapping wing mechanism did not happen in the absence of other biological factors. In the resource constrained field of microrobotics, it is possible that mimicking the flight of an insect may necessitate a specific design space. For that reason, we believe that developing new flight mechanisms for flying microrobots may lead to otherwise impossible applications, platforms, and discoveries. The thrust for our flying robot will be generated electrohydrodynamically (EHD); that is, by using the flow of ions to generate a momentum transfer in the opposite direction of desired flight. The flow of neutral air through the collector electrode due to collisions with the moving ions represents the net momentum transfer of the system, analogous to how a propeller accelerates some mass of air to produce thrust. EHD thrusters are silent, have a high thrust to weight ratio due to requiring only sparse electrodes to produce useful work, and are mechanically robust due to their lack of moving parts.

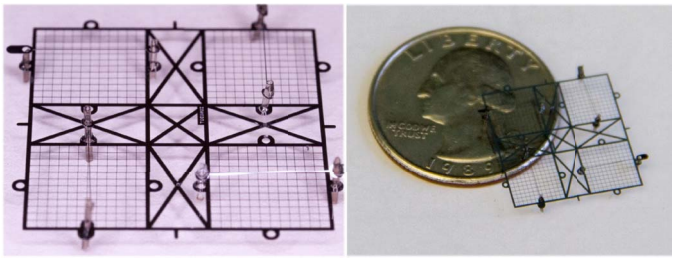

Fig. 1. These "quad-thrusters" are made of microfabricated silicon electrodes and fused silica capillary tubes and assembled by hand. They are 1.8cm x 1.8cm, 10mg, with four individually addressable electrode sets, and a 1mm electrode gap. They should be capable of producing around 1mN of force for a thrust to weight ratio of about 10.

The "ion wind" effect was studied as early as 1700 and explored by minds such as Newton, Faraday, and Maxwell [5]. Modern understanding of the effect was formalized in seminal papers by Christenson, Moller, and Robison [6] [7]. While these provided explanations and derivations of the governing physical models, little was done in the application space until decades later. In the 1960s the effect was studied for use in aircraft, even being featured on the cover of *Popular Mechanics* in 1964, but the conclusion was that EHD thrust was ill-suited for these goals. Today the most widely known use of EHD thrust may be with the "lifter" model popular with students and hobbyists. The lifter is on the order of one square meter, typically constructed from balsa wood and aluminum foil, and can provide sufficient lift for take off when connected to a high voltage (30kV) power supply.

A. Electrohydrodynamic Force

It is possible to derive an expression for EHD thrust in terms of ion current starting from the Coulomb force acting on a volume of ions occupying a gap [8]. This one dimensional model assumes that electrode cross sectional area is large compared to the gap length, d.

$$F = \int \rho E dV = \int \rho E A dx = \int \frac{Id}{\mu V A} \frac{V}{d} A dx = \frac{Id}{\mu} \quad (1)$$

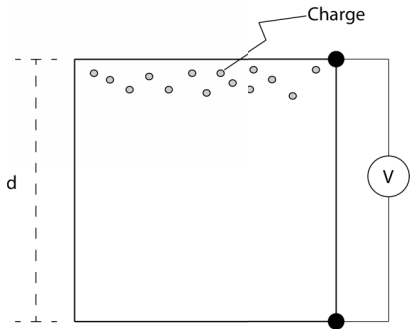

Fig. 2. Reference figure for understanding the ionic force derivation. The charged particles will drift under the influence of the electric field, which has a magnitude of $\frac{V}{d}$.

Where I is ion current and μ is the ion mobility. A more useful two-dimensional model can also be derived from the Coulomb electric force and some fundamental definitions.

$$Q_0 = CV_{drive} = \epsilon_0 L V_{drive} \quad (2)$$

$$Q_{gap} = \alpha Q_0 \quad (3)$$

In the preceding equations we have assumed that the ions (charges) are injected into a cubic capacitive gap by some mechanism. This then yields the α coefficient which has a maximum value of 9/8, as dictated by the Mott-Gurney law (4) which states that there is a space charge saturation limit of the conduction current density.

$$J = (9/8)\epsilon \mu V^2 / L^3 \quad (4)$$

Finally, electrostatic force on the ions injected into the gap is given in Equ. 5. Note that this is force acting on the ions; direct translation of this to thrust requires that all momentum is transferred in the preferred thrust direction by ion-neutral collisions.

$$F = Q_{gap} E_{drive} = \alpha \epsilon_0 L V_{drive} E_{drive} = \alpha \epsilon_0 L^2 E_{drive}^2 \quad (5)$$

With thrust efficiency in terms of Newtons per Watt of:

$$I = Q\frac{V}{d} = \alpha \epsilon_0 \frac{A}{d^3} \mu V^2 \quad (6)$$

$$P = IV = \alpha \epsilon_0 \frac{A}{d^3} \mu V^3 \quad (7)$$

$$\frac{F}{P} = \frac{d}{\mu V} = \frac{1}{\mu E} \quad (8)$$

The electrical efficiency equation (8) shows that, at the breakdown field in air of $3\frac{MV}{m}$ and using an ion mobility in air of $2 * 10^{-4} \frac{m^2}{Vs}$, the efficiency will be approximately $2\frac{mN}{W}$. Assuming a constant ion mobility and that all momentum is transferred in the preferred direction, this efficiency is a theoretical minimum for ion thrust.

To illustrate this design space we can plot the EHD theoretical thrust versus efficiency curve (in Newtons per Watt), shown in Fig. 3. This plot is not meant to be a conclusive comparison between flying microrobots; it serves to show that EHD has the potential to provide high thrust compared to biomimetic designs at the cost of efficiency. Conversely, simply lowering the applied DC voltage and hence decreasing the ion drift field can increase the efficiency while decreasing the thrust to levels similar to that achieved by flapping wing microrobots. It should be noted that at identical efficiency levels, there will theoretically be less thrust than from a flapping wing mechanism. We stipulate that the various other benefits of EHD thrust, e.g. silent flight and high thrust to weight ratio, still make it an attractive alternative.

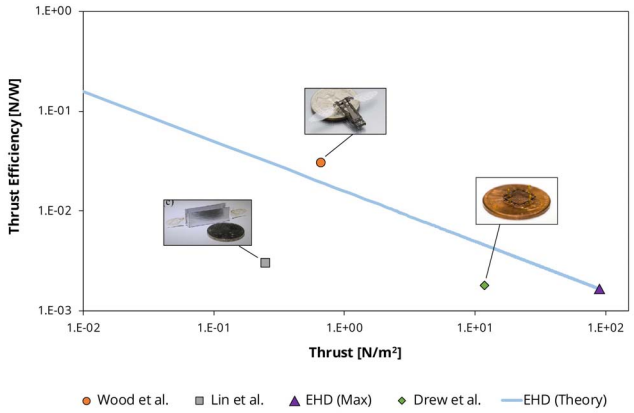

Fig. 3. Efficiency in terms of $[N/W]$ versus thrust in terms of $[N/m^2]$ for various examples of flying microrobots, including previous work from this group [9]. The theoretical curve for EHD thrust is also shown to illustrate how the two metrics trade off. Points derived from values given in work by Wood [4] and Yan et al. [3] should be taken as approximations. The plot shows that, without taking into account metrics like ease of fabrication/design and thrust to weight ratio, EHD thrust has the ability to achieve similar efficiency and thrust values as biomimetic designs.

B. Corona Discharge

An electrohydrodynamic thruster requires both a way to accelerate ions to produce force as well as a way to generate them. A common method for producing the ions is corona discharge, which has been adopted for commercial applications including electrostatic precipitators and mass spectrometers. Corona discharge as a mechanism to produce an ion drift current has been separately studied at electrode gaps down to hundreds of micrometers [10].

Corona discharge is an atmospheric-pressure ionization process characterized by a self-sustained plasma localized around a charged conductor, the emitter, and ionic current flowing to a second electrode, the collector. The corona region is generated primarily by strong electric fields arising due to geometric effects, e.g. a small diameter wire or sharp point [11]. The magnitude of the discharge is typically space-charge

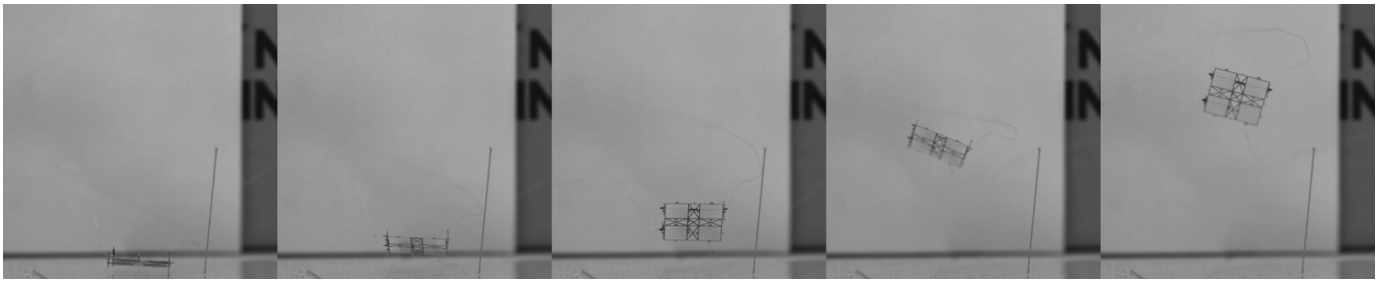

Fig. 4. Takeoff of a microfabricated ionocraft captured at 1000fps. At about 2400V it took flight silently. The flight ended in around a second when the power connection became tangled with the collector grid, leading to an arc.

limited, with the polarity determined by whether high voltage is applied to the emitter ("positive corona discharge") or the collector ("negative corona discharge").

The critical field criterion for corona discharge inception has been widely used and experimentally verified since the 1920s [12]. Using it, a corona onset potential V_0 can be defined for a given geometry. For a wire-to-plane geometry, the corona inception voltage is given by:

$$V_0 = g_0 r_0 \left(1 + \frac{0.301}{\sqrt{r_0}}\right) ln\left(\frac{2d}{r_0}\right) \tag{9}$$

Where g_0 is the breakdown field strength equal to about 30kV/cm for air, r_0 is the radius of the emission wire in centimeters, and d is the distance between the wire and the plane in cm. This equation has been simplified to assume standard temperature and pressure as well as an ideal smooth wire. The ability to microfabricate electrodes with small radii of curvature and to lithographically define small electrode gaps allows for favorable scaling of the corona discharge initiation point.

II. Related Work

Electrohydrodynamic thrust has been revisited as a flight mechanism in recent research. Masuyama et al. verified the theoretical framework of EHD thrust and concluded through extensive experimentation that thrust-to-power ratios are comparable with many conventional propulsion mechanisms [13]. Further work concluded that due to the experimentally measured thrust densities on the order of $10Nm^{-3}$, EHD propulsion is most suited for small UAV applications [14]. It should be noted that thrust densities measured in this work are two orders of magnitude higher than this value.

A large amount of work has been performed simulating and optimizing corona discharge-based EHD systems. The typical approach combines the critical field criterion established by Peek with the Kaptzov hypothesis, which stipulates that the electric field on the corona emitter surface remains constant at Peek's critical value even as applied voltage increases. Surface charge density and subsequently the space charge region can then be solved for, yielding a numerical solution for ion current due to drift. Typical simulation performed in this manner agrees to within about 10% with experimental values [15]. Combining this approach with a diffuse species collision model and a flow model yields a simulated measure of air flow; this approach has also been verified experimentally [16].

Miniaturized EHD devices have been used as low power convection coolers and for ion spectrometry tools. A microfabricated EHD cooling device has been demonstrated with an operating voltage around 1000V [17]. Corona discharge in air has been found to be a relatively stable, repeatable, and high current ionization source for ion mobility spectrometry [18]. Microfabricated corona discharge based devices have shown promise as portable airborne particle analyzers and separators [19].

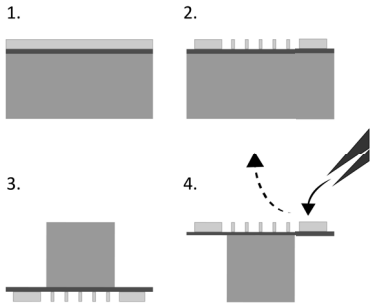

Fig. 5. The simple two mask silicon-on-insulator (SOI) process to fabricate the silicon electrodes. First the $40\mu m$ device silicon is patterned. The wafer is flipped and loosely bonded to a handle wafer using a thermally conductive grease. The 500 μm handle silicon is aligned, patterned, and then etched to plasma dice the individual devices. Finally, tweezers are used to physically remove the electrodes, breaking the buried oxide in the process. The electrodes are placed into a vapor HF etcher to clear the remaining oxide.

III. Fabrication and Assembly

Electrode geometries were chosen based on a combination of lessons learned from previous efforts to create meso-scale EHD thrusters (e.g. limits of repeatable gap scaling for a given emitter radius), availability of a stable fabrication process with the given wafer properties, and feasibility of hand assembly (e.g. minimum size to handle with tweezers). Devices are fabricated in a two mask silicon-on-insulator (SOI) process and individually plasma diced. The active electrode material is all device-side silicon, allowing for a high thrust to weight ratio as the force is a predominantly two dimensional effect. The process flow is depicted in Fig. 5. After the backside deep

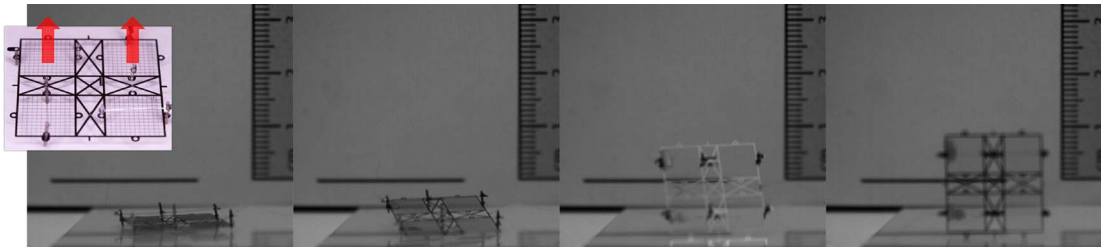

Fig. 6. By applying voltage to only two of the four grids we can control roll/pitch of the robot. In this video, captured at 1000fps, the ionocraft flips over its center axis when the two rear thrusters are actuated at about 2400V.

reactive ion etch, the devices are physically removed from the wafer with tweezers and etched with vapor HF to clear the buried oxide layer. Corona discharge is a strong function of electrode geometry; care must be taken in designing the electrodes to prevent early breakdown, reverse corona (where a plasma is formed around the collector), and wasted area. Exterior corners are filleted and only rounded shapes are used in non-functional area, e.g. near the dielectric standoff attachment points.

Fused silica capillary tubing with an inner radius of about $400\mu m$ and a wall thickness of $25\mu m$ is used for the dielectric posts that set the distance between the two electrodes. The device is designed so that they can be fabricated in a stack - a rendered depiction of the device assembly is shown in Fig. 7. An aluminum jig is used during the assembly process to assist with placement and alignment of the silica tubes. An assembled ionocraft is about 10mg and 1.8cm by 1.8cm (see Fig. 1). It takes roughly thirty minutes to assemble by hand.

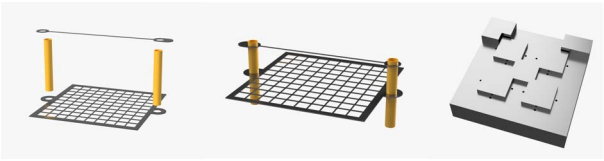

Fig. 7. Fused silica capillary tubes are inserted vertically through slots in the microfabricated silicon electrodes and secured with UV-curable epoxy applied via probe tip. A machined aluminum fixture (far right) provides help with alignment and stability. Tabs on the emitter wire and collector grid (latter not shown) provide a place to attach the power connections using silver epoxy applied via probe tip.

IV. Experimental Methods and Results

During electrical characterization the quad-thruster is weighted down by glass cover slips so it remains stable. High voltage was supplied to the emitter wire by a Gamma High Voltage 10kV supply and current was measured by a benchtop ammeter connected to the collector grid. The power supply is current limited to protect the ammeter. The results are shown in Fig. 8 for both a full quadthruster, for two grids, and for one grid of the same device. Using Equation 1 with the loss factor for a similar electrode geometry found in [9] of 50%, a peak force for the quad-thruster of about 1mN is expected, corresponding to a thrust to weight ratio of 10.

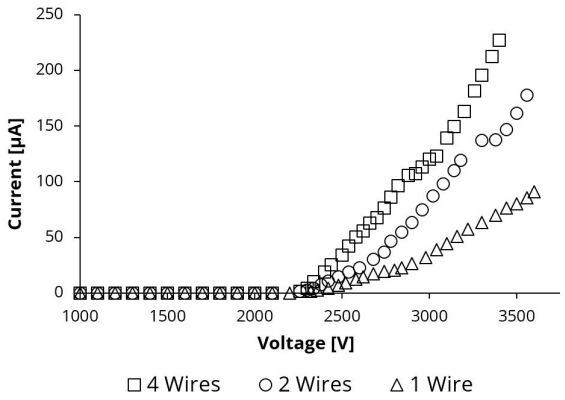

Fig. 8. Electrical characterization of a quad-thruster with number of actuated wires varied. Calculated corona onset voltage is 2309V with a standard deviation of 50V. Measured currents agreed with geometric prediction (e.g. one wire produces one fourth the current of four wires at a given voltage) to within about 5% on average. Tests concluded when an arc occurred, destroying the wire.

Using $60\mu m$ diameter copper wires as the power connections the device was actuated in front of a high speed camera. At about 2400V the ionocraft took flight, reaching a peak attitude of around 5cm before the instability of its attitude caused a power wire to touch the collector grid. This flight is shown in Fig. 4. From this video a peak acceleration of about 2 gravities can be calculated, corresponding to a force of about $200\mu N$, far below the theoretical maximum force these devices should be able provide. During the video the voltage was being slowly increased by hand and, due to the high thrust to weight ratio, the device took off and subsequently crashed before the voltage could be increased to the levels used to measure the maximum thrust point.

The goal of using four individually addressable electrode sets is to allow for attitude control similar to that of a quadcopter. As an initial feasibility test, only two of the four thrusters were actuated. As shown in Fig. 6, this created a moment around the center axis and the ionocraft flipped over as predicted. The question of how to control yaw remains open. A traditional quadcopter controls yaw by coupling torque from its rotors to produce a net moment around only one axis; the EHD thruster presented here has no analagous torque component. One possibility is to angle the emitter electrode along the vertical axis in order to produce horizontal force,

although this would lead to decreased vertical force.

V. Conclusions and Next Steps

While takeoff and the feasibility of attitude control has been demonstrated, the path to an autonomous ionocraft requires advancement on a number of fronts. Light weight and low power sensing, computation, control, and communications modules all need to be integrated; although the ionocraft has a high thrust to weight ratio, it is still a relatively low amount of force and we expect the microrobot to have a highly constrained mass budget. To save on payload mass, it may be possible to use an ion thruster as both a sensor and an actuator; changes in ion mobility and hence output force can be related to humidity or pressure. The electrostatic precipitation effect can clean the air while providing thrust for the robot to fly [20].

A controller needs to be implemented that takes into account the EHD thrust nonlinearities; beyond requiring further characterization of the thrust mechanism itself, it will also require development of low mass and high speed high-voltage switching circuitry. Previous work has demonstrated SOI CMOS circuits with NMOS breakdown voltages above 50V and PMOS close to 100V, which could be increased further with process optimization or worked around in circuit design [21]. Because body dynamics increase in speed with decreased size, it may be necessary to implement some form of passive stability into the mechanical design to decrease the required controller bandwidth [22].

Finally, everything needs to be powered by a high energy density, high-voltage battery array. Thin, high aerial density printable lithium ion batteries have been demonstrated that could potentially power an ionocraft given further thickness reduction to increase discharge rate [23]. The operating voltage must be decreased to minimize series resistance losses and potential breakdown events in the power array; this will require further optimization of the electrode sets and likely changing the assembly process to allow for lithographically defined electrode gaps.

It is possible to imagine using the microfabricated atmospheric ion thruster presented here as a component in other microrobotic platforms. Previous research has demonstrated lift to drag ratios in excess of 10 from centimeter-scale wings [24]; ion thrusters could be used like jets under similar wings to increase their effective lift [25]. Their planar geometry and high thrust to weight ratio means it is also possible they could be incorporated onto walking platforms for short range "hops" over unfavorable terrain.

Acknowledgment

The authors would like to thank the entire Pister group and Swarm Lab. All fabrication was performed at the UC Berkeley Marvell Nanolab.

References

[1] A. M. Flynn, "Gnat robots (and how they will change robotics)," *MIT Artificial Intelligence Laboratory, Working Papers*, 1987.

[2] R. J. Wood, B. Finio, M. Karpelson, K. Ma, N. O. Pérez-Arancibia, P. S. Sreetharan, H. Tanaka, and J. P. Whitney, "Progress on picoair vehicles," *The International Journal of Robotics Research*, vol. 31, no. 11, pp. 1292–1302, 2012.

[3] X. Yan, M. Qi, and L. Lin, "Self-lifting artificial insect wings via electrostatic flapping actuators," in *Micro Electro Mechanical Systems (MEMS), 2015 28th IEEE International Conference on*. IEEE, 2015, pp. 22–25.

[4] R. J. Wood, "The first takeoff of a biologically inspired at-scale robotic insect," *IEEE transactions on robotics*, vol. 24, no. 2, pp. 341–347, 2008.

[5] M. Robinson, "A history of the electric wind," *American Journal of Physics*, vol. 30, no. 5, pp. 366–372, 1962.

[6] E. A. Christenson and P. S. Moller, "Ion-neutral propulsion in atmospheric media." *AIAA Journal*, vol. 5, no. 10, pp. 1768–1773, 1967.

[7] M. Robinson, "Movement of air in the electric wind of the corona discharge," *Transactions of the American Institute of Electrical Engineers, Part I: Communication and Electronics*, vol. 80, no. 2, pp. 143–150, 1961.

[8] L. Pekker and M. Young, "Model of ideal electrohydrodynamic thruster," *Journal of Propulsion and Power*, vol. 27, no. 4, pp. 786–792, 2011.

[9] D. Drew, D. S. Contreras, and K. S. J. Pister, "First thrust from a microfabricated atmospheric ion engine," in *Micro Electro Mechanical Systems (MEMS), 2017 30th IEEE International Conference on*. IEEE, 2017.

[10] R. Tirumala, Y. Li, D. Pohlman, and D. Go, "Corona discharges in submillimeter electrode gaps," *Journal of Electrostatics*, vol. 69, no. 1, pp. 36–42, 2011.

[11] J.-S. Chang, P. A. Lawless, and T. Yamamoto, "Corona discharge processes," *IEEE Transactions on plasma science*, vol. 19, no. 6, pp. 1152–1166, 1991.

[12] F. W. Peek, *Dielectric phenomena in high voltage engineering*. McGraw-Hill Book Company, Incorporated, 1920.

[13] K. Masuyama, "Performance characterization of electrohydrodynamic propulsion devices," Ph.D. dissertation, Massachusetts Institute of Technology, 2012.

[14] C. K. Gilmore and S. R. Barrett, "Electrohydrodynamic thrust density using positive corona-induced ionic winds for in-atmosphere propulsion," in *Proc. R. Soc. A*, vol. 471, no. 2175. The Royal Society, 2015, p. 20140912.

[15] K. Adamiak and P. Atten, "Simulation of corona discharge in point–plane configuration," *Journal of electrostatics*, vol. 61, no. 2, pp. 85–98, 2004.

[16] L. Zhao and K. Adamiak, "Ehd flow in air produced by electric corona discharge in pin–plate configuration," *Journal of electrostatics*, vol. 63, no. 3, pp. 337–350, 2005.

[17] A. O. Ong, A. R. Abramson, and N. C. Tien, "Electrohydrodynamic microfabricated ionic wind pumps for thermal management applications," *Journal of Heat Transfer*, vol. 136, no. 6, p. 061703, 2014.

[18] M. Tabrizchi, T. Khayamian, and N. Taj, "Design and optimization of a corona discharge ionization source for ion mobility spectrometry," *Review of scientific instruments*, vol. 71, no. 6, pp. 2321–2328, 2000.

[19] B. Chua, A. S. Wexler, N. C. Tien, D. A. Niemeier, and B. A. Holmen, "Electrical mobility separation of airborne particles using integrated microfabricated corona ionizer and separator electrodes," *Journal of Microelectromechanical Systems*, vol. 18, no. 1, pp. 4–13, 2009.

[20] Y. Zhuang, Y. J. Kim, T. G. Lee, and P. Biswas, "Experimental and theoretical studies of ultra-fine particle behavior in electrostatic precipitators," *Journal of electrostatics*, vol. 48, no. 3, pp. 245–260, 2000.

[21] C. L. Bellew, S. Hollar, and K. S. J. Pister, "An soi process for fabrication of solar cells, transistors and electrostatic actuators," in *TRANSDUCERS, Solid-State Sensors, Actuators and Microsystems, 12th International Conference on, 2003*, vol. 2. IEEE, 2003, pp. 1075–1078.

[22] M. Piccoli and M. Yim, "Passive stability of a single actuator micro aerial vehicle," in *Robotics and Automation (ICRA), 2014 IEEE International Conference on*. IEEE, 2014, pp. 5510–5515.

[23] A. E. Ostfeld, A. M. Gaikwad, Y. Khan, and A. C. Arias, "High-performance flexible energy storage and harvesting system for wearable electronics," *Scientific reports*, vol. 6, 2016.

[24] P. J. Kunz, "Aerodynamics and design for ultra-low reynolds number flight," Ph.D. dissertation, Stanford University, 2003.

[25] D. S. Drew, B. Kilberg, and K. S. J. Pister, "Future mesh-networked pico air vehicles," in *Unmanned Aircraft Systems (ICUAS), 2017 International Conference on*. IEEE, 2017.